Micro-Positioning of Linear Piezoelectric Motors Based on a Learning Nonlinear PID Controller

H. Zhou[1] K. K. Tan and T. H. Lee
Department of Electrical and Computer Engineering
National University of Singapore
Singapore 117576

Abstract

In this paper, a learning nonlinear PID controller is developed for vaguely modeled nonlinear systems under significant disturbance and noise. The control scheme is generic in nature, but it is applied specifically to micro positioning of linear piezoelectric motors in this paper. Mathematical models for the piezoelectric motor and the associated friction phenomenon are provided and verified in the simulation and experimental results provided. These results also highlight the good motion control performance achieved from the control scheme.

1 Introduction

Piezoelectric actuators are innovative manipulators that have shown a high potential in applications requiring manipulation within the sub-micrometer or even nanometer range. Initial applications have been mainly to provide accurate short travel motion (e.g. microscope focusing device [1]), but efficient co-operated uses of multiple piezoelectric elements have expanded the application domain to include longer travel applications as in micro-assembly (e.g. MEMS), precision metrology and process automation.

There are two main classes of linear piezoelectric motors (LPM), according to their structures and driving principles. The first class works on a direct-drive principle. Deformations of a piezoelectric element are directly used to drive the load for precision positioning [2]. The second class of LPM operates instead on an indirect-drive principle. In [3][4], inchworm types of indirect-drive piezoelectric motors are presented. The generated force and maximum moving speed are very low with this configuration, although there is no physical limitation to travel length and high resolution of 5nm has already been achieved [3]. Another type of indirect-drive piezoelectric motor is the ultrasonic motor or acoustic motors which use piezoelectric components to generate ultrasonic waves and produce a linear motion [5][6]. The characteristics of ultrasonic piezo motors are: high resolution, unlimited travel, wide dynamic range of velocity, hold stability at power off, and a small compact structure.

While the piezoelectric actuator has high potential for application in ultra-precision motion control systems, the highly nonlinear features associated with the dynamics of these elements are challenges to how efficiently these potentials can be realized. For the direct-drive type, hysteresis is the main part of the nonlinear characteristics [8]. For the indirect-drive type, friction has been identified as the main problem to be addressed [5]. From the viewpoint of the control system, friction poses an interesting and challenging dilemma to the control problem. On one hand, it provides the primary transfer mechanism to bring about the motion, and on the other hand, it opposes the realization of precision motion control.

In this paper, we propose a learning-enhanced nonlinear PID control strategy for an indirect-drive, ultrasonic-type of LPM. The control scheme does not require an accurate model, but it is capable of yielding good motion tracking performance, as evident in the simulation study and experiments presented in the paper. The control system is robust to the presence of disturbances and measurement noises, using high performance differentials tracking and state observer systems. Above all, the structure of the control system is simple and directly intuitive to the practitioners. These features are clearly demonstrated in the simulation and real-time experiment results documented in the paper.

2 Modeling of LPM

Fig. 1 shows the principal structure of an ultrasonic-type LPM considered in this work. The stator vibrator is fitted with bending and longitudinal piezoelectric actuators. They are driven by two electrical sources of identical frequency, but with a phase difference that is carefully controlled. At the vibration tip, an elliptical motion is thus created, resultant of the elliptical and longitudinal motion. A vibration circuit working at resonant frequency is used to cause the longitude

[1]Corresponding author: elezhx@nus.edu.sg

and bending ceramic components to vibrate. The velocity and direction of the moving plate can be adjusted by changing the shape and phase of the ellipse. Thus, there is a complicated function of frictional force acting during a complete motion cycle.

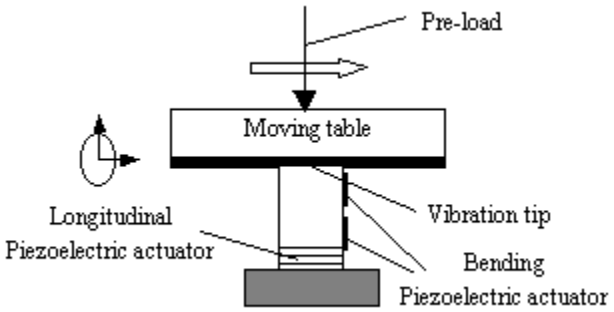

Figure 1: Ultrasonic-type LPM

Friction is inevitable in many practical systems and its effect on machine performance has been demonstrated by a number of researchers [11]. It is a highly complicated process to attempt to build an explicit mathematical friction model for the LPM because friction plays a dual role: it does not simply contribute to the nonlinear dynamics (e.g. dead zone) of the LPM, but it also serves as the driving force for the moving part. For the purpose of simulation, a conventional and generally acceptable Tustin friction model [11] will be adopted.

The LPM can be expressed as a second order nonlinear differential equation:

$$m\ddot{y} = u - K_{vf} - f(\dot{y}) \tag{1}$$

where m denotes the total moving mass, y denotes the position, u denotes the applied force, c denotes the viscous damping coefficient. $K_{vf}\dot{y}$ thus represents the viscous friction and $f(\dot{y})$ represents the combined effects of negative viscous and the Coulomb friction. The Tustin model for $f(\dot{y})$ is given by:

$$f(\dot{y}) = (a_0 + a_1 e^{-a_2|\dot{y}|})sgn(\dot{y}) \tag{2}$$

where a_0, a_1, a_2 are the three parameters of the model and $sgn(.)$ represents the standard sign operator.

First order estimates of K_f (force constant) and K_{vf} (velocity damping coefficient) can be obtained from simple step experiments as:

$$\begin{cases} K_{vf} = m/\tau, \\ K_f = |V_\infty| K_{vf}/U_{in} \end{cases} \tag{3}$$

where U_{in} is the step size of a step input signal; V_∞ is the corresponding steady-state velocity of the step response and τ is the system time constant obtained from the same step response.

3 Controller Design

The conventional PID controller is a widely used industrial controller that uses a combination of proportional, integral and derivative action on the control error to form the output of the controller. It is known that the linear combination of these components can at most achieve a compromised performance in terms of system response speed and stability. A nonlinear combination can provide additional degree of freedom to achieve a much improved system performance [9]. However, this improvement can only be achieved at the expense of higher complexity in the controller. Artificial intelligence approaches can alleviate some of the difficulties by fusing a priori information or expert knowledge into the control design.

Another prominent difficulty with PID control is in the practical implementation of the derivative action. Derivative action provides a degree of predictive control capability to yield faster response without excessive an overshoot/undershoot, its practical merits are often questionable. In the presence of measurement noise or rapidly changing disturbance signals, it is often unclear as to whether derivative action will give any control improvement. In some cases, a first-order filter is used in conjunction with the differentiator. In other cases, derivative action may just be switched off altogether. In this section, we adopt a nonlinear differential tracker (DT) to replace the differential component of the PID controller for more effective and robust performance in the presence of noise and other uncertainties. The DT can be further expanded to serve as an Extension States Observer (ESO). The ESO can act as a soft sensor of general disturbance signals arising in the control system. A feedforward control action may then be taken in response to the observed disturbance before it affects the system performance.

Finally, the nonlinear PID control system is augmented with a repetitive learning control scheme for further performance enhancement when the system executes repetitive operations. The error states from previous iterations are used in a PID-type learning law to produce an additional feedforward control output. As we will show in the simulation study and experiments, the learning feedforward control component can achieve arbitrarily good performance. It only requires the feedback control system to be stable, although a well-tuned feedback controller will help to expedite the learning convergence.

3.1 Nonlinear Differential Tracker (DT)

Suppose a system described by:

$$\begin{cases} \dot{z}_1 = z_2, \\ \dot{z}_2 = f(z_1, z_2) \end{cases} \tag{4}$$

has solutions meeting the requirements: $z_1(t) \to 0, z_2(t) \to 0$ when $t \to \infty$. Then, for any boundary integrable functions $v(t)$, the solution, $x_1(t)$, of the system [9]:

$$\begin{cases} \dot{x}_1 = x_2, \\ \dot{x}_2 = R^2 f(x_1 - v, x_2/R) \end{cases} \tag{5}$$

will satisfy

$$\lim_{R\to\infty} \int_0^T |x_1(t) - v(t)| dt = 0 \tag{6}$$

where R is a constant.

For the second order time optimized switch system,

$$\begin{cases} \dot{z}_1 = z_2, \\ \dot{z}_2 = -sign(z_1 + z_2|z_2|/2) \end{cases} \tag{7}$$

from any initial states, the states $z_1, z_2 \to 0$, when $t \to \infty$.

Therefore, the system described by:

$$\begin{cases} \dot{x}_1 = x_2, \\ \dot{x}_2 = -R \cdot sign(x_1 - v(t) + x_2|x_2|/2R) \end{cases} \tag{8}$$

can be used as a high performance differential tracker (DT) of the tracking signal $v(t)$ and the differential component in conventional PID controller can be replaced by the DT for a more robust performance Fig.2 shows the performance of differential tracker, where $v(t) = 20\sin(\omega t)$ and it is disturbed by a white noise with the maximum amplitude of 0.5. For clear illustration, the differential signals obtained respectively by DT and general PID controller are normalized by ω in Fig.2. It can be seen that the differential tracking performance of DT is much better than a pure differentiator.

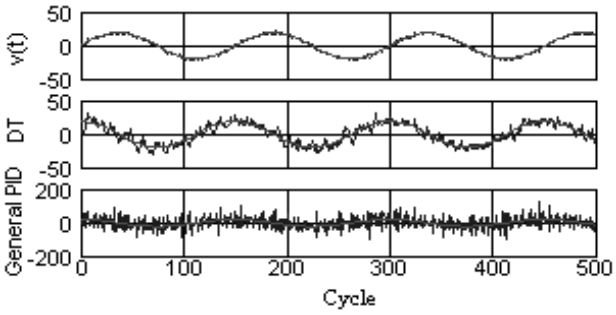

Figure 2: Differential Signals

3.2 Nonlinear extension states observer (ESO)

Suppose the system model is described by:

$$y^{(n)} = f(\cdot) + d(t) + ku(t) \tag{9}$$

where $y^{(n)} = f(y, y^{(1)}, \cdots, y^{(n-1)}, t)$, $d(t)$ is the disturbance signal, k is a control coefficient. $u(t)$ and $y(t)$ denote the input and output of the system respectively. A nonlinear state observer is designed to estimate system states, as well as an extension state [10]. The nonlinear observer for the system is described as:

$$\begin{cases} \dot{z}_1 & = z_2 - g_1(z_1 - y) \\ \dot{z}_2 & = z_3 - g_2(z_1 - y) \\ & \vdots \\ \dot{z}_{n-1} & = z_n - g_{n-1}(z_1 - y) \\ \dot{z}_n & = z_{n+1} - g_n(z_1 - y) + ku(t) \\ \dot{z}_{n+1} & = -g_{n+1}(z_1 - y) \end{cases} \tag{10}$$

where, $z_1, z_2, \cdots, z_n$ are the estimated values of $y, \dot{y}, \cdots, y^{(n-1)}$ respectively, $g_1 \sim g_{n+1}$ are nonlinear compensation functions. The state, z_{n+1} , is called the extension state. If system is stable, for suitable functions, $g_1 \sim g_{n+1}$, it follows:

$$\lim_{t\to\infty} |f(t) + d(t) - z_{n+1}| = \epsilon \tag{11}$$

where ϵ is an arbitrarily small positive constant. Equation 11 implies that the extension state, z_{n+1}, is the estimated value of $f(t) + d(t)$, which is really the uncertain value of the system to be estimated. The $fal(.)$ function (see next part) will be used as the nonlinear compensation functions, $g_i, i = 1, 2, \cdots, n+1$.

3.3 Nonlinear PID controller

With two second-order DTs, a nonlinear PID controller can be constructed as in Fig.3.

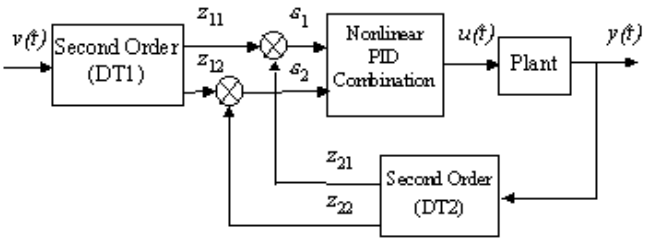

Figure 3: Nonlinear PID Controller

DT1 and DT2 are two DTs which track input signal $v(t)$, output signal $y(t)$ and their differentials. Variables, $z_{11}, z_{21}, z_{12}, z_{22}$, are their estimated values. e_1 and e_2 denote the position and velocity tracking errors respectively. Analogous to general linear PID controller, the nonlinear combination of the error signals can be expressed as:

$$u(t) = k_p fal(\epsilon_1, \alpha, \delta) + k_i \int \epsilon_1 dt + k_d fal(\epsilon_2, \alpha, \delta) \tag{12}$$

where k_P, k_i, k_d are the PID control coefficients, $fal(.)$ is a selected nonlinear function described by:

$$fal(\epsilon, \alpha, \delta) = \begin{cases} |\epsilon|^{\alpha} & |\epsilon| > \delta \\ \epsilon/\delta^{1-\alpha} & |\epsilon| \leq \delta \end{cases} \quad (13)$$

where α, δ are constants.

A linear input-output relationship is effectively used when $\epsilon \leq |\delta|$ to provide a smoother control action when e is near zero. Using a third-order ESO, an improved version of the nonlinear PID controller (Fig.4) can be constructed which can deal more effectively with disturbance signals arising.

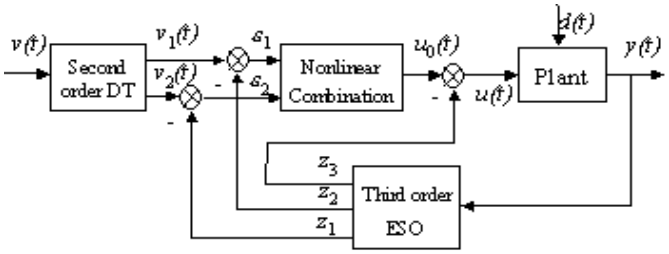

Figure 4: Nonlinear State Feedback Controller

The equation for nonlinear combination can be expressed as:

$$u_0(t) = \beta_1 fal(\epsilon_1, \alpha, \delta) + k_i \int \epsilon_1 dt + \beta_2 fal(\epsilon_2, \alpha, \delta) \quad (14)$$

The control law is thus:

$$u(t) = (u_0(t) - z_3)/k \quad (15)$$

where z_3 is provided by the state estimator, equation 10.

3.4 Repetitive learning control

In many applications, the LPM can be subject to periodic reference input signal. For example, for a precision CNC elliptical piston-turning machine, a high speed, high precision linear actuator is needed to track a $40Hz$ periodic signal with a stroke of $0.5mm$ [13]. For high performance engine pistons, a maximum contour error of $4um$ is required.

In this part of the paper, the feasibility of applying the discrete time repetitive learning control technology as an additional control component for the LPM to improve the response to periodic reference inputs will be explored. As shown in Fig.5, the learning controller represents an additional feedforward control branch to the stabilized system that is controlled by the nonlinear PID controller described in the earlier subsections.

A PID-type learning law[12] is used for learning controller. The learning law is described by:

$$u_{k+1}(i) = u_k(i) + f(e_k(i), \sum_i e_k(i), de_k(i)/dt) \quad (16)$$

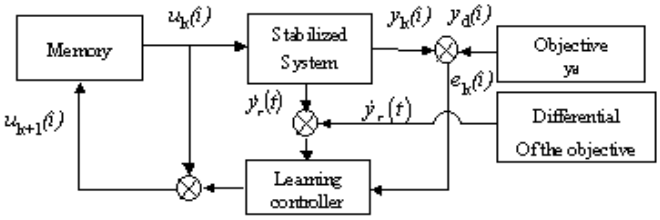

Figure 5: Repetitive Learning Control

where $u_{k+1}(i)$ is the learning control signal generated during the $k+1$ cycle for the ith sampling point; $f(.)$ is the correction function for the learning value. A proposed PID-type correction function is given by:

$$f(\cdot) = k_P e_k(i{+}1) + k_I \sum_{n-1}^{i+1} + k_D[e_k(i{+}1) - e_k(i)], i \in [0, N{-}1] \quad (17)$$

where N is the number of sample points within a cycle.

4 Simulation and Experiment

To illustrate the effectiveness and applicability of the control scheme developed, simulation and real-time experiments are carried out on a single axis linear stage manufactured by Steinmeyer Company. The stage is driven by a SP-8 piezoelectric motor, which is manufactured by Nanomotion. The DSPACE DS1102 control card is used in conjunction with MATLAB and SIMULINK for the experiment.

From system identification experiments, the system model is identified to be:

$$\begin{cases} m\ddot{y} = 3.076u - 39.13\dot{y} - 6.142sgn(\dot{y}) - f(\dot{y}) - f_d \\ f(\dot{y}) = 4.921e^{-89.56|\dot{y}|}sgn(\dot{y}) \end{cases} \quad (18)$$

4.1 Simulation results

A sinusoidal reference signal, $v(t) = 1.5\sin(30\pi t)$, is used for the simulation. In addition, a disturbance signal, $0.3sgn\sin(60\pi t)$, is simulated. The simulation results based on the use of a linear PID controller and the nonlinear PID controller with the ESO are shown in Fig.6 and Fig.7 respectively. For a fair comparison, the linear PID controller is fine tuned to yield optimal performance. The nonlinear controller with the ESO exhibits a improved tracking and disturbance rejection performance compared to the linear PID controller. The maximum tracking error is reduced by 50%.

Finally, a learning controller is added to improve the tracking precision. Fig.8 and Fig.9 show the control

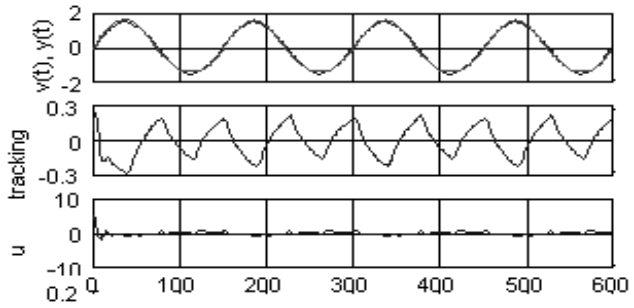

Figure 6: Linear PID Control under disturbance, $d(t)$

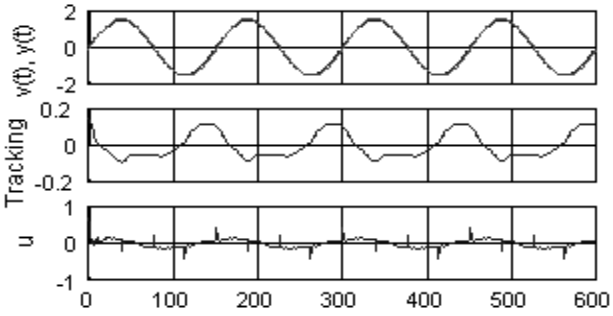

Figure 7: Nonlinear PID with ESO under $d(t)$

results with the learning controller augmented. A maximum tracking error of ± 0.002 can be achieved after 30 cycles in the absence of disturbances and ± 0.01 in the presence of disturbances. The error curve is now completely different from the one of Fig.7 due to the additional learning control component. Although it is still periodic, the frequency is changed.

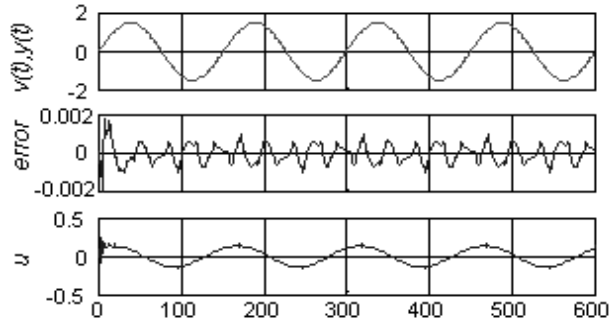

Figure 8: Learning Nonlinear Controller

The error convergence speed is dependent on the PID parameters of the learning controller. In fact, the coefficients K_p, K_i, K_d can be changed from one cycle to another to improve the system convergence performance. Thus, for example, larger parameters for the learning controller may be applied to obtain high convergence speed initially, and they may be subsequently reduced to obtain higher tracking precision.

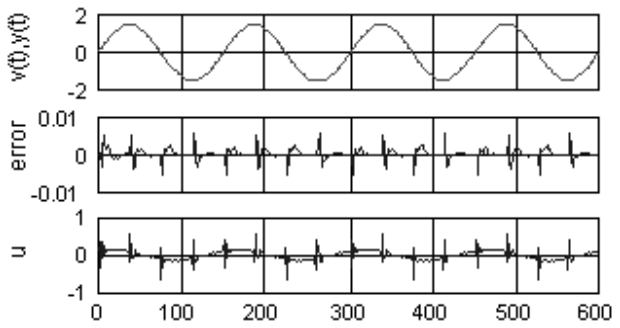

Figure 9: Learning Nonlinear Controller under $d(t)$

4.2 Experimental results

The real-time experimental results obtained on the physical system are provided categorically below.

(a)DT performance

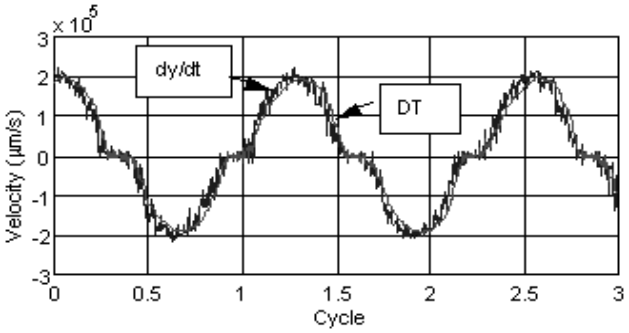

Figure 10: Differential Signals

Fig.10 shows the differential output signals obtained using the DT and a pure differentiator (dy/dt) when a white noise disturbance $d(t)$ appears at the input. Although improvement is observed in the DT which gives a smoother differential signal, it is not very significant as the mechanical system acts as an inherent high frequency filter to the input signal. An interesting observation is that the experimental results in Fig.10 are very similar to the simulation results (Fig.2), thereby verifying to some extent the adequacy of the model adopted.

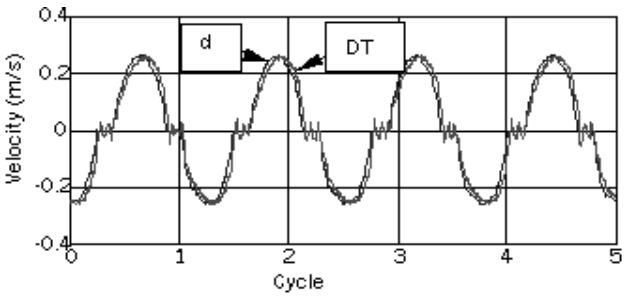

Figure 11: Differential Signals from DT, d is the ideal signal

When the disturbance appears at the output, the im-

provement using DT is clearly evident from the respective signals in Fig.11. A clean differential signal is obtained from the DT. From the pure differentiator (dy/dt), the profile of the differential signal is almost completely lost in noise.

(b)Nonlinear PID controller performance

Fig.12 shows the system tracking errors resultant of using the nonlinear PID controller. The tracking error from the nonlinear PID controller is about 50% that from the linear PID controller. The maximum error occurs at the transition point when the motion changes direction and the full dosage of friction is experienced.

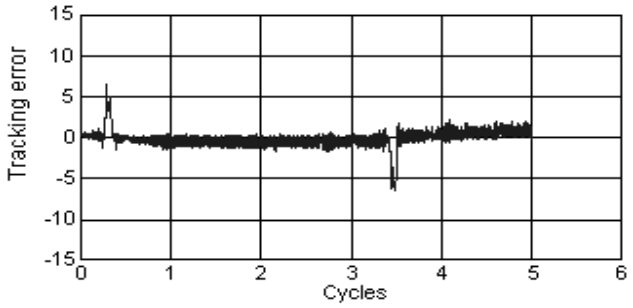

Figure 12: Tracking Error-Nonlinear PID control

(c) Learning Nonlinear PID performance

Next, a PID learning controller is added to the nonlinear PID controller. Fig.13 shows the results. The tracking error in Fig.13 is obtained at the $20th$ learning cycle, which is a further 50% of the tracking error obtained from a non-learning NPID controller. The sign of the control output is changed when the motion switches direction.

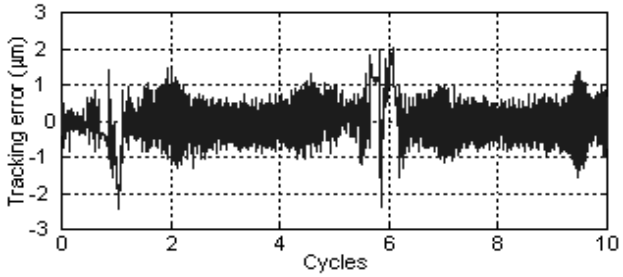

Figure 13: Tracking Error - 20th Cycle

5 Conclusion

In this paper, we demonstrated the effectiveness of a nonlinear PID controller augmented with a learning strategy when applied to precision motion control of piezoelectric actuators. The nonlinear PID controller is composed of two differentiator trackers that can yield high quality differential signal in the presence of disturbances and measurement noise. With an additional learning controller, the maximum position tracking error can be further reduced by a factor of approximately 50%.

References

[1] A. Visscher and and J.W. Coenders, "Linear piezo motor," *Internal Report CTR595-93-0147,* Philips Centre for Manufacturing Technology, 1993.

[2] T. Moriwaki and E. Shamoto, "Ultraprecision feed system based on walking drive," *Annals of the CIRP,* vol. 46, no.1, pp. 505-508, Jan. 1997

[3] B. Zhang and Z. Zhu, "Developing a linear piezomotor with nanometer resolution and high stiffness," *IEEE/ASME Transactions on Mechatronics,* vol. 2, no. 1, pp. 22-29, Mar. 1997

[4] M. J. Edward, "Piezoelectric/Magnetostrictive resonant inchworm motor development," *Ph.D. dissertation,* George Washington University, Nov. 1994

[5] M. Takahashi, M. Kurosawa, etc., "Direct friction driven surface acoustic wave motor," *The 8th International Conference on Solid-State Sensors and Actuators,* Stockholm, Sweden, pp. 401-404, Jun. 1995

[6] M. Kurosawa and S. Ueha, "Hybrid transducer type ultrasonic motor," *IEEE Transactions on Ultrasonics, Ferroelectrics and Frequency Control,* vol. 38, no. 2, Mar. 1991

[7] D. Newton, E. Garcial and G. C. Horner, "A linear piezoelectric motor," *Smart Materials and Structures,* no. 6, pp. 295-304, 1997

[8] P. Ge, M. Jouaneh, "Tracking control of a piezoceramic actuator," *IEEE Control System Magazine,* vol. 4, no. 3, pp. 209-216, May. 1996

[9] H. Jingqing, "A new type of controller: NLPID," *Control and Decision,* vol. 9, no. 6, pp. 401-407, Nov. 1994 (In Chinese)

[10] H. Jingqing, "Extension state observer for a type of uncertain objectives," *Control and Decision,* vol. 10, no. 1, pp. 85-88, Feb. 1995 (In Chinese)

[11] B. Armstrong-Helouvry, P. Dipont, C. Canudas de Wit, "A survey of models, analysis tools and compensation methods for the control of machines with friction," *Automatic,* vol. 30, pp. 1083-1138, 1994

[12] D. Kim, S. Kim, "An iterative learning control method with application for CNC machine tools," *IEEE Transactions on Industry Application,* vol. 32, no. 1, pp. 66-72, 1996

[13] H. Zhou, L. Zhang and X. Wang, etc., "Repetitive control and its application to linear servo unit for CNC machining of elliptical pistons," *IEEE ICIT'96, Shanghai,* pp. 630-633, 1996